CMEs and Active Regions on the Sun

Grzegorz Michalek

Astronomical Observatory of Jagiellonian University,30-244 Cracow, Poland

Seiji Yashiro[1,2]

[1] *NASA Goddard Space Flight Center, Greenbelt, MD 20771, USA*
[2] *The Catholic University of America, Washington, DC 20064, USA*

Abstract

The relationship between active regions (ARs) and coronal mass ejections (CMEs) is studied. For this purpose a statistical analysis of 694 CMEs associated with ARs was carried out. We considered the relationship between properties of the CMEs and ARs characterized using the McIntosh classification. We demonstrated that CMEs are likely to be launched from ARs in the mature phase of their evolution when they have complex magnetic field. The fastest and halo CMEs can be ejected only from the most complex ARs (when an AR is a bipolar group of spots with large asymmetric penumbras around the main spot with many smaller spots in the group). We also showed that the wider events have a tendency to originate from uncomplicated magnetic structures. This tendency was used for estimation of the real angular widths of the halo CMEs. The probability of launching of fast CMEs increases together with increase of the complexity and size of ARs. The widest, but slow, CMEs originate from the simplest magnetic structure which are still able to produce CMEs. Our results could be useful for forecasting of space weather.

Keywords: Sun; solar activity; coronal mass ejection

1. Introduction

Coronal mass ejections (CMEs) are large expulsions of magnetized plasma from the Sun. The first CME was detected on 14 December 1971 by the

Email addresses: michalek@oa.uj.edu.pl (Grzegorz Michalek), seiji.yashiro@gmail.com (Seiji Yashiro[1,2])

white-light coronagraph onboard NASA's OSO-7 satellite (Tousey, 1973). It is well known that they are responsible for major geomagnetic storms leading to numerous effects in the ionosphere, atmosphere, and on the ground (*e.g.* Gopalswamy, Yashiro and Akiyama, 2007). The CMEs originate from closed magnetic structures which are commonly observed in active regions (ARs) on the Sun. During solar maxima, large number of AR (consisting of spot groups) appear. Sunspot groups can have a large variety of shapes and sizes. Despite such a diversity of shapes and sizes, there have been at least three major attempts to classify morphological properties of sunspot groups. The Zurich sunspot classification was introduced by Waldmeier (1947). More recently, it has been replaced by a method derived by McIntosh (1990). A classification of the ARs based on their magnetic properties was also developed (Smith and Howard, 1967). The McIntosh Sunspot Classification Scheme (MSCS), which is commonly used, is based on three descriptive codes 'Zpc' (where 'Z' is the modified Zurich classes, 'p' describes the penumbra of the main spot, and 'c' describes the distribution of spots in a group). The scheme attempts to describe a typical evolutionary sequence of sunspot groups. The first code, using seven categories (A, B, C, D, E, F, and H), defines the length of sunspot groups. Length is defined in absolute heliographic degrees and is free from projection effect. The successive letters represent sunspot groups with increasing sizes. For example, the 'A' means an unipolar group with no penumbra while the 'F' represents the largest possible sunspot group with angular span $>15^{\circ}$. The last letter 'H' identifies an unipolar group with penumbra in the final phase of evolution. The second code using six categories (X, R, S, A, H, and K), characterizes the type of largest spot in a group. It describes the size of penumbra, symmetry of penumbra and umbrae within that penumbra. The successive letters describe the main spots with increasing size and complexity of the penumbra. For example, the letter 'X' means the main spot without penumbra while the letter 'K' describes the large main spot with asymmetric penumbra with angular span $>2.5^{\circ}$. The last code, using four categories (X, O, I, and C), specifies spottedness in the interior of a sunspot group. Additionally it gives information about appearance of strong spot near the line of polarity inversion lying between the main and follower spots. The successive letter describe sunspot groups with increasing number of spots inside. For example, the letter 'X' represents a unipolar group while the letter 'C' identifies the spot group populated with many strong spots with at least one interior spot possessing mature penumbra. These three components of the MSCS are objective indicators of size,

stability and complexity of sunspot groups. About 35% of all the ARs are classified as AXX or BXX. Bornmann and Shaw (1994) derived a flare rate per day for each of the three parameters of the MSCS. They demonstrated that the average flare rate increases with increasing complexity of the ARs. Bornmann and Shaw (1994) studied a five-year period of observations to determine similarities among the different classes of the ARs. Studying evolution of ARs it was also possible to determine the most frequent transitions between different classes of the MSCS (Bornmann and Shaw, 1994). They also determined occurrence rates for different classes of the MSCS.

The source regions of CMEs have been intensively studied (*e.g.* Lara, 2008). It is known that sheared magnetic structures observed in photospheric magnetograms are likely to erupt (Ambastha, Hagyard, and West, 1993; Gopalswamy, 2003). In soft X-ray images the photospheric shears have S and reverse S-shaped features (Rust and Kumar, 1996). These sigmoidal structures are more eruptive than the non-sigmoidal regions (Canfield, Hudson, and McKenzie, 1999). It is assumed that an eruptive active region is characterized by: a strong magnetic field, a sheared neutral line and a global net current (Falconer, 2001). Recently, Yashiro *et al.* (2007) considered the productivity of CMEs and flares from two active regions. They found that the active regions could produce different number of flares and CMEs. The first active region was CME-rich with 72% association with flares while the second was CME-poor with an association rate only 14%.

The MSCS parameters serve as proxies for the magnetic properties of ARs and are likely to be correlated with CMEs-productivity. In this article, we present a statistical analysis of CMEs associated with ARs. Using a large set of data, 694 pairs of related CMEs and ARs, we examine the magnetic structures of the ARs to see if this can account for productivity and properties of CMEs. This is the goal of this article. In Section 2, the data used for this study are described. A statistical analysis of properties of CMEs associated with ARs is presented in Section 3. Finally, conclusions and discussion are presented in Section 4.

2. Data

In this section the procedure applied for the creation of the list of ejections is presented. For our analysis we used two databases. The list of CMEs was taken from the SOHO/LASCO CME catalog (www.cdaw.gsfc.nasa.gov/CME_list). This catalog includes a full description of CMEs within the range of $2-30$

solar radii from the Sun. For purposes of the present study, from this catalog, the angular widths and velocities obtained from linear fits to height – time plots were used. We investigated all the CMEs within the period of the time 2001 – 2004. The description of ARs is provided by the Space Weather Prediction Center (SOLAR REGION SUMMARY, www.swpc.noaa.gov). To associate these two phenomena, two conditions must be fulfilled. There must be a temporal coincidence between them and they must be located in the same quadrant of the solar disk. To eliminate backside events, EIT movies were checked for the presence of any signatures of initiation of CMEs from the solar disk. Backside and questionable CMEs were excluded from further considerations. The applied procedure allowed us to select 644 pairs of CMEs and ARs.

3. Results

3.1. Active Regions

In Figure 1 the distributions of the three codes of MSCS for the ARs associated with the CMEs, the ARs associated with halo events (events appearing around the entire occulting disk) and a general population of the ARs considered by Borman and Shaw (1994) are presented. We consider independently (on separate figures) halo events because they constitute physically different group of CMEs (Michalek, Gopalswamy and Yashiro, 2003). Halo CMEs when they are directed toward the Earth could be geo-effective. The diagrams clearly indicate that CMEs are ejected only from the ARs that achieve complex structures. The first column of panels (Figure 1 (a), (d) and (g)) shows the frequency distributions of the first code of MSCS for the three sub-samples of the ARs. The ARs are usually not very elongated structures (Figure 1 (g)). 93% all of the ARs is observed as A (0.20-numbers placed next to the letters are relative frequencies of occurence for a given class of ARs), B(0.18), C(0.17), D(0.16) or H(0.22) subclasses of the MSCS. Only 7% of all the ARs seem to be much more elongated (E, F subclasses). This tendency changes when we investigate the ARs associated with the CMEs (Figure 1 (a)). The CMEs are likely to be ejected from the elongated bipolar ARs (D(0.33), E(0.30), F(0.25)). This tendency is even more significant for the ARs associated with the halo CMEs (Figure 1 (d)).

The frequency distributions of the second code of MSCS are displayed in the second column (Figure 1 (b), (e) and (h)). From this figure it is clear that the main spots in the case of the general population of ARs are usually

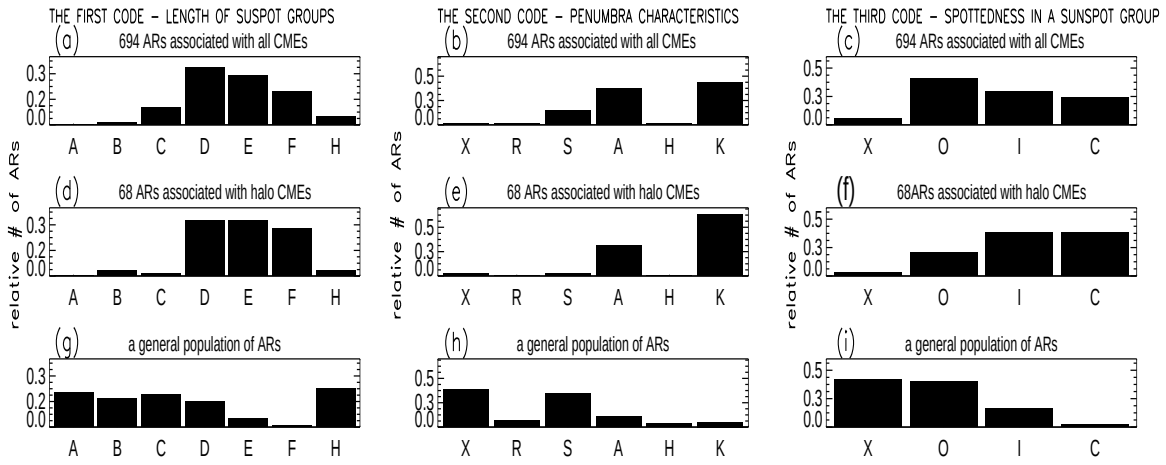

Figure 1: The distribution of three codes of MSCS for ARs associated with CMEs (top row; (a), (b), and (c) panels), ARs associated with halo events (middle row; (d), (e) and (f) panels), and a general population of ARs considered by Borman and Shaw (1994) (bottom row; (g), (h), and (i). The first code, using seven categories (A, B, C, D, E, F, and H), defines the length of sunspot groups. The successive letters, from A to F, represent sunspot groups with increasing angular sizes. The last letter 'H' identifies an unipolar group with penumbra in the final phase of evolution. The second code using six categories (X, R, S, A, H, and K), characterizes the type of largest spot in a group. The successive letters, from X to K, describe the main spots with increasing size and complexity of penumbra. The third code, using four categories (X, O, I, and C), specifies spottedness in the interior of a sunspot group. The successive letter, from X to C, describe sunspot groups with increasing number of spots inside.

encompassed by small and not complex penumbras (Figure 1 (h)). 76% of all the ARs is observed as X (0.39) and S (0.37) subclasses of the MSCS. On the other hand, the ARs which are related to the CMEs have mostly asymmetric penumbras around the main spots (Figure 1 (b) and (e)). As many as 85% of the ARs is observed as A(0.40), K(0.45) subclasses of the MSCS. It is interesting that these CMEs are rarely ejected from the ARs with the main spot encompassed by a large but symmetric penumbra (H - class). This interesting result suggests that a volume of magnetic structures is not the most important factor deciding about the ejection of CMEs. The most important factor determining ejections is the complexity of magnetic field. The frequency distributions of the last code of MSCS are displayed in the third column of Figure 1 ((c), (f), and (i) panels). A general population of the ARs (Figure 1 (i)) is dominated by uncomplicated subclasses (X(0.41), O(0.39)) of the MSCS. On the other hand, the ARs associated with the CMEs are likely to have many small spots indicating that they have the complex magnetic structures. As many as 95% of these ARs are observed as the O(0.40), I(0.31), C(0.24) subclasses of MSCS.

Halo CMEs are of interest due to their increased geo-effectiveness (Michalek, Gopalswamy and Yashiro, 2003). These events seem to be faster and wider than the whole population of CMEs (*e.g.* Michalek, Gopalsamy, and Yashiro, 2003). The distributions of the codes of MSCS for the ARs associated with the halo CMEs are shown in the middle row of panels (Figure 1 (d), (e) and (f)). The data clearly indicates that the halo CMEs can be launched only from extremely complex ARs. To launch a halo CME, beside central location on the solar disk, an active region must: be a bipolar group (D, E, or F), have an asymmetric penumbra around the leading spot (A, K) and have many other spots within the group (I, C).

3.2. Velocity of CMEs

In Figure 2, the distributions of CME velocity for the first code of MSCS of the associated ARs are displayed. The two subclasses of the ARs (A and B) have been dropped in the figure because we do not observe any CMEs associated with them. Coronagraphic observations of CMEs are subject to projection effects (Gopalsamy *et al.*, 2001; Michalek *et al.*, 2006) which affect velocity measurements. To examine how projection effects affect our study, we analyzed separately limb CMEs (left panel). These CMEs, originating from the solar limb (with solar longitudes $> 60^{\circ}$), remain in the plane of the sky through the duration of observation and are almost free from projection

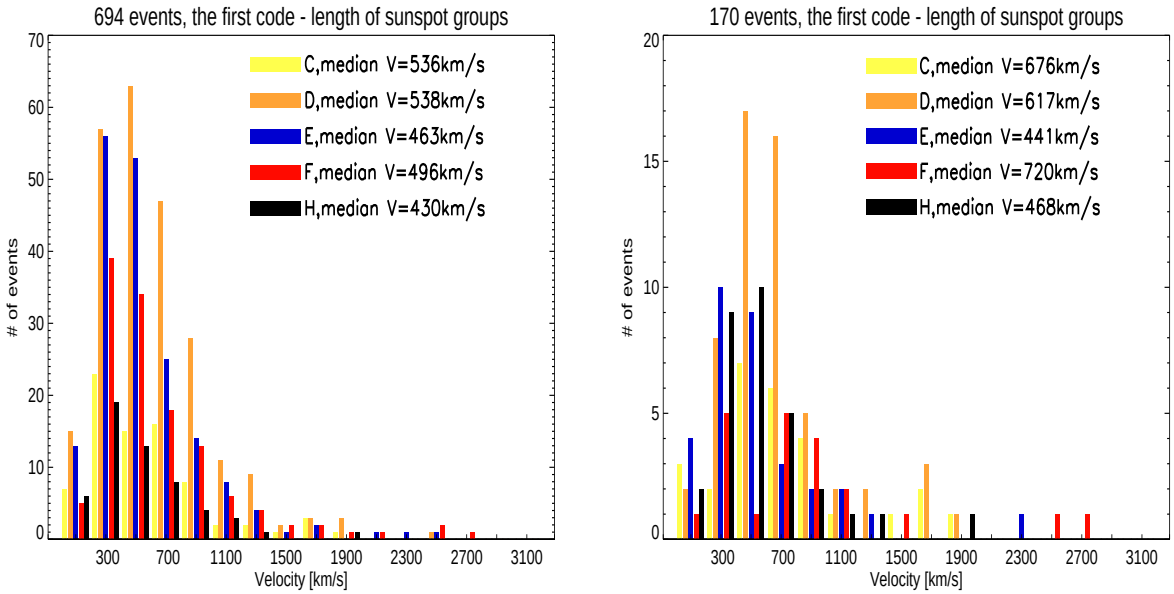

Figure 2: Histograms showing the distributions of CME velocity for the first code of MSCS of the associated ARs. The first code, using seven categories (A, B, C, D, E, F, and H), defines the length of sunspot groups. The successive letters, from A to F, represent sunspot groups with increasing angular sizes. The last letter 'H' identifies an unipolar group with penumbra in the final phase of evolution. The left and right panels are for all and limb events, respectively. Median values are indicated at the right – top corners.

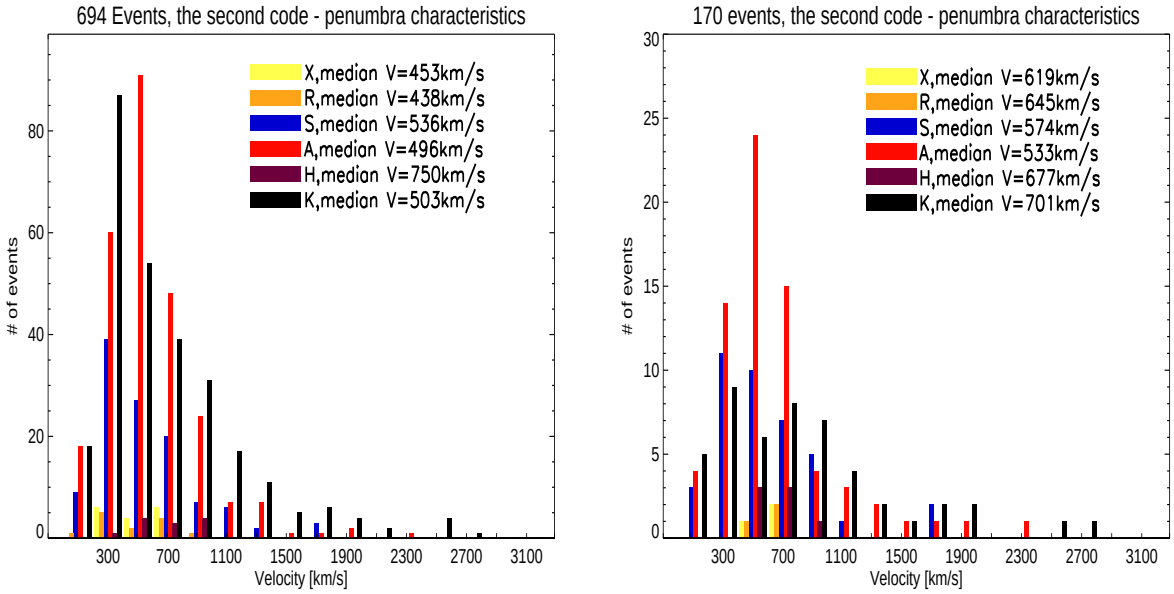

Figure 3: Histograms showing the distributions of CME velocity for the second code of MSCS of the associated ARs. The second code using six categories (X, R, S, A, H, and K), characterizes the type of largest spot in a group. The successive letters, from X to K, describe the main spots with increasing size and complexity of penumbra. The left and right panels are for all and limb events, respectively. Median values are indicated at the right – top corners.

effects. From the figure it is clear that fast CMEs (v>1000 km s^{-1}) are likely to be launched when the ARs are achieving large sizes and are in the main phase of their evolution (C, D, E, F sub-classes of the first code). The fast CMEs could be also expelled when a bipolar group starts to disappear (H - category). The largest median velocity have CMEs associated with the F - subclass of the ARs (the median velocity for the limb events is equal to 720 km s^{-1}). The two fastest CMEs (v>2000 km s^{-1}) were associated with very large ARs (F - category). What is interesting, we recorded one fast event ($v = 1913$ km s^{-1}) surprisingly associated with an unipolar AR (HKX). However, during the ejection of CME this AR was still very complicated. It had the CKX configuration a day before the CME initiation. For space – weather forecasting it is important to remember that disappearing active regions, still having complicated magnetic structures, are able to generate the fast mass ejections. Figure 3 shows the distributions of CME velocity for the second code of MSCS of the associated ARs. The diagrams demonstrate

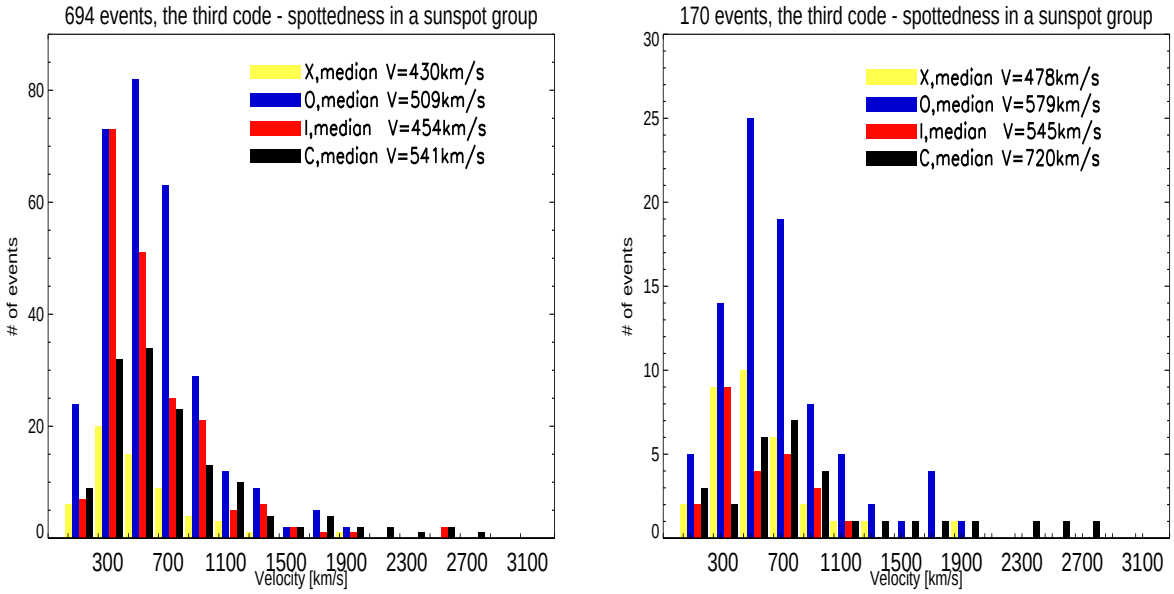

Figure 4: Histograms showing the distributions of CME velocity for the third code of MSCS of the associated ARs. The third code, using four categories (X, O, I, and C), specifies spottedness in the interior of a sunspot group. The successive letter, from X to C, describe sunspot groups with increasing number of spots inside. The left and right panels are for all and limb events, respectively. Median values are indicated at the right – top corners.

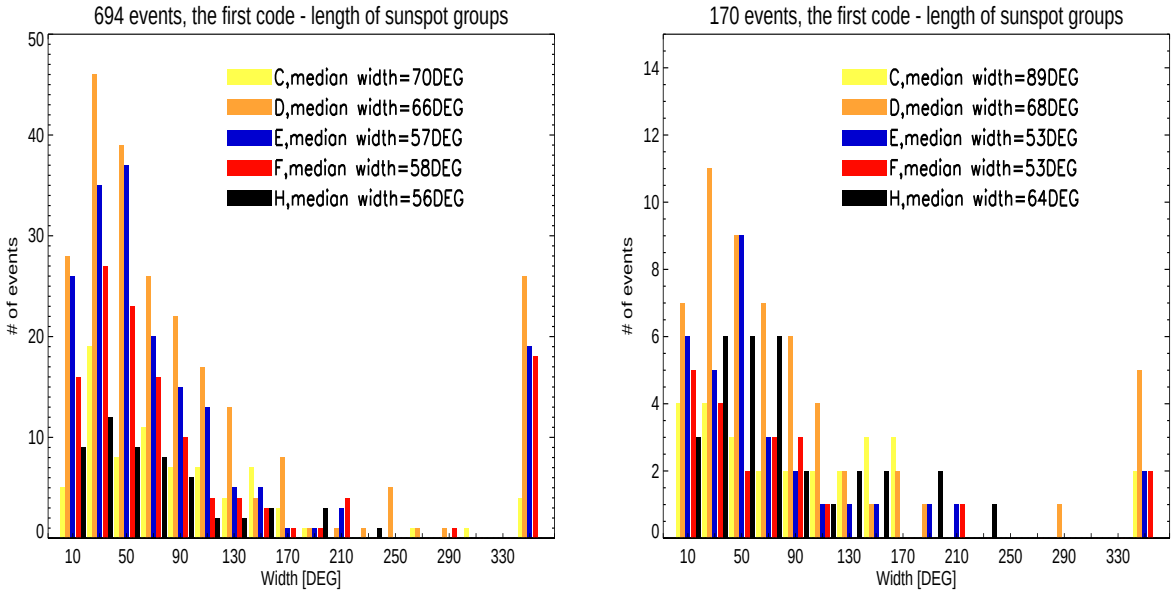

Figure 5: Histograms showing the distributions of CME width for the first code of MSCS of the associated ARs. The first code, using seven categories (A, B, C, D, E, F, and H), defines the length of sunspot groups. The successive letters, from A to F, represent sunspot groups with increasing angular sizes. The last letter 'H' identifies an unipolar group with penumbra in the final phase of evolution. The left and right panels are for all and limb events, respectively. The left and right panels are for all and limb events, respectively. Median values are indicated at the right – top corners.

that the fast CMEs are associated with the S, A, and K subclasses of ARs. The largest median velocity have CMEs related to the K subcategory of ARs (the median velocity for the limb events is equal to 701 km s^{-1}). Figure 4 displays the distributions of CME velocity for the third parameter of MSCS of the associated ARs. These histograms show that the fast CMEs are likely to be ejected from the ARs having many small spots (C and O subcategories). The largest median velocities, almost two times larger with comparison to the others events, have CMEs associated with the C subcategory of ARs (the median velocity for the limb events is equal to 720 km s^{-1}).

3.3. Width of CMEs

The second most important parameter characterizing CMEs is their angular width. Figure 5 shows the distributions of CME width for the first code of MSCS of the associated ARs. As in the case of the velocity consid-

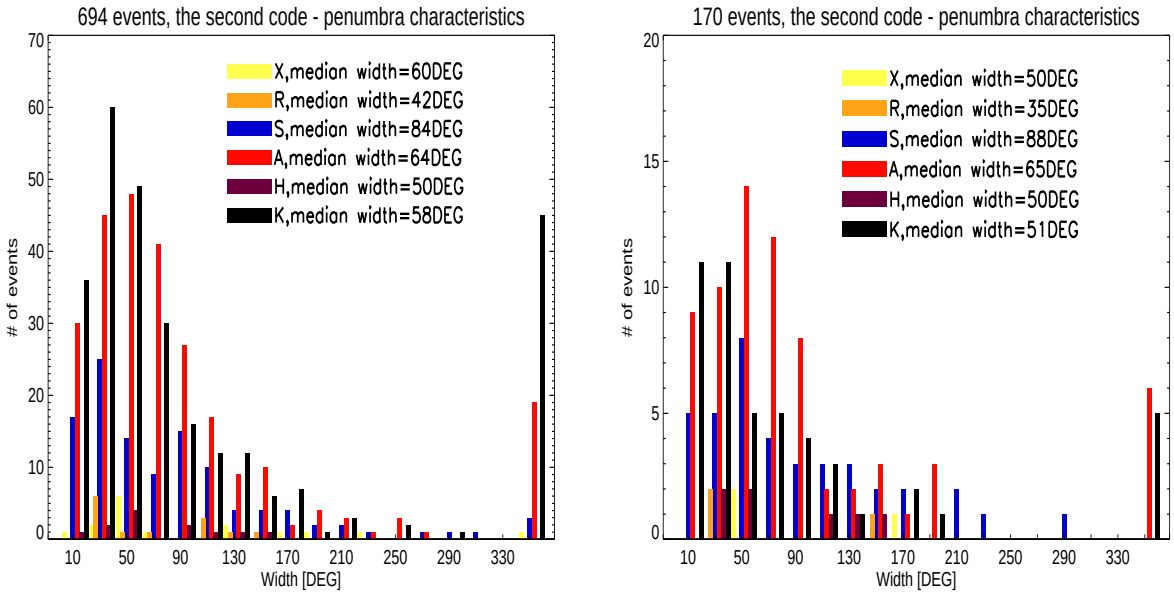

Figure 6: Histograms showing the distributions of CME width for the second code of MSCS of the associated ARs. The second code using six categories (X, R, S, A, H, and K), characterizes the type of largest spot in a group. The successive letters, from X to K, describe the main spots with increasing size and complexity of penumbra. The left and right panels are for all and limb events, respectively. Median values are indicated at the right – top corners.

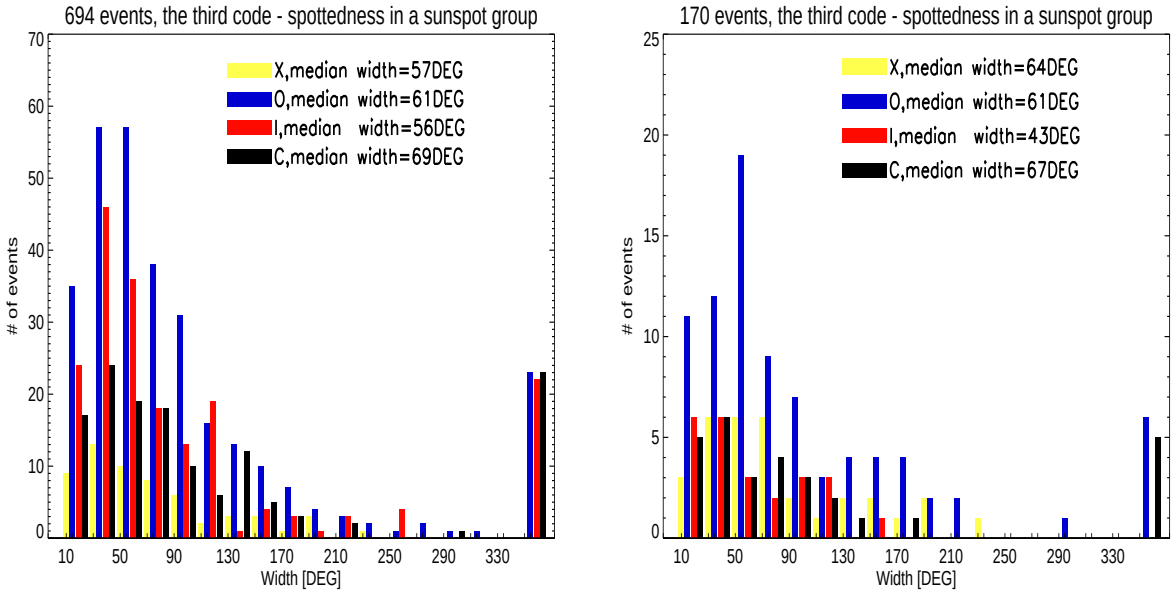

Figure 7: Histograms showing the distributions of CME width for the third code of MSCS of the associated ARs. The third code, using four categories (X, O, I, and C), specifies spottedness in the interior of a sunspot group. The successive letter, from X to C, describe sunspot groups with increasing number of spots inside. The left and right panels are for all and limb events, respectively. Median values are indicated at the right – top corners).

erations, the A and B subcategories of ARs are not included in the figure. The widest population of CMEs is associated with not very elongated ARs (C subcategory). The median width for these CMEs, for the limb events, is 89°. It is almost two times larger in comparison with the CMEs related to the E and F subcategories of ARs. A similar trend is observed for the second code of MSCS. Figure 6 shows the distribution of CME widths for the second code of the MSCS of the associated ARs. The widest CMEs are likely to be ejected from the ARs described by S-code of MSCS (the median width for the limb CMEs is 88°). The widest CMEs have a tendency to be launched from the ARs not having very large main spots encompassed by a tiny symmetric penumbras. Finally, Figure 7 shows the distributions of CME width for the third parameter of the MSCS of the associated ARs. Although formally the widest ejections are associated with the most complex active areas (the largest median width is achieved for the C subcategory of ARs) we cannot say that this is a significant trend. For this code of the MSCS the distributions of width of the associated CMEs differ little and have similar

median values. This means that the angular width of CMEs does not depend significantly on the compactness of the associated ARs.

Halo CMEs (width = 360°) are particulary interesting. Due to projection effects, they appear in coronagraphs around the entire occulting disk. As can be seen in Figures 5, 6, and 7, their association with the ARs is different than for the whole population of CMEs. They are likely to be launched from complex ARs. The halo events are ejected from the ARs which have: large magnetic structures (D, E and F subcategories), asymmetric spot encompassing the main spot in a group (H and A subcategories) and have many small spots (O and C subcategories). As it is clear they behave differently as the population of the widest ejections.

4. Summary and Discussion

In this article we considered properties of the ARs associated with CMEs. We demonstrated that CMEs are likely to be ejected from the ARs consisting of the large bipolar structures (C, D, E, F) with asymmetric penumbrae around the largest spots (A, K) and many smaller spots in the group (O, I, C). CMEs are not launched from ARs in the beginning phase of their evolution (A and B subcategories for the first code of the MSCS which define small sunspots with no penumbra). Occasionally, ejections can be generated by the ARs that are in the terminal phase of their evolution (H subcategory for the first code of the MSCS). For space weather forecasting, it is important to remember that the decaying active regions (H subcategory-a unipolar sunspot with penumbra) could still have a complicated magnetic structure and are able to generate the extremely fast mass ejections. It is also very interesting that CMEs are rarely launched from the extended ARs when their leading spots are encircled by symmetric penumbras (H-subcategory for the second code of the MSCS). We recorded only seven CMEs (1% of all the ARs associated with the CMEs) associated with this class of ARs.

The fast (v>1000 kms^{-1}) CMEs, which are potentially geo-effective, can be ejected only from the most complex ARs having following configurations: D, E, F (the first code of the MSCA- large bipolar sunspot groups with penumbra on both ends); A, K (the second code of the MSCS- asymmetric penumbras around the largest spots), and I, C (the third code of the MSCS- numerous spots between the leading and following portions of the group). The fastest CMEs were initiated most frequently by the ARs having the MSCS configuration FKC (an elongated bipolar sunspot group with asym-

metric penumbras on both ends and populated with many strong spots) The angular width, the second most important parameter characterizing CMEs, behaves differently to the velocity of the CMEs. Wider ejections are generated by less complex active regions. Please note that this trend is not true for halo CMEs for which we can not determine angular widths from coronagraphic observations and they are not used for these considerations. This tendency is the most clearly present when we consider the two first code of the MCSC. The widest CMEs are associated with the not very elongated ARs (C subcategory for the first code of the MSCS) with symmetric penumbrae encompassing the largest spot (S subcategory for the second code of the MSCS). The angular width of CMEs does not depend significantly on the compactness of the ARs (the third code of the MSCS).

The halo CMEs, which are directed to the Earth, have special interest. For these events we are not able to determine angular widths from observations. They are, as fast events, ejected from the most complicated ARs as was demonstrated in the previous sections. Conversely, we have also shown that wide CMEs originate form simpler magnetic structures. This implies that the halo events should have smaller angular widths in comparison with the widest population of CMEs. The median width of the halo events should be in the range of angles between 60° and 89°. This indirect estimation of their average width complements our knowledge about these events.

Acknowledgements
Grzegorz Michalek was supported by MNiSW through the grant N203 023 31/3055 and NASA (NNX08AD60A).

References

Ambastha, A.; Hagyard, M. J.; West, E. A. Evolution and Flare-Associated Magnetic Shear Variation in Solar Active Regions. American Astronomical Society, 24th SPD Meeting, 07.05; Bulletin of the American Astronomical Society, 25, 1189, 1993.

Bornmann, P.L., Shaw, D. Flare rates and the McIntosh active-region classifications. Solar Phys. 150, 127-146, 1994.

Bornmann, P.L., Kalmbach, D., Kulhanek, D.McIntosh active-region class similarities and suggestions for mergers. Solar Phys. 150, 147-164, 1994.

Canfield, R.C., Hudson, H.S., McKenzie, D.E.Sigmoidal morphology and eruptive solar activity. J. Geophys. Res. 26, 627-630, 1998.

Falconer, D.A. A prospective method for predicting coronal mass ejections from vector magnetograms. J. Geophys. Res. 106, 25185-25190, 2001.

Gopalswamy, N. Coronal mass ejections: Initiation and detection. Adv. Space Res. 31, 869-881, 2003.

Gopalswamy, N., Yashiro, S., Kaiser, M.L., Howard, R.A., Bougeret, J.-L. Radio Signatures of Coronal Mass Ejection Interaction: Coronal Mass Ejection Cannibalism? Astrophys. J. 548, L91-L94, 2001.

Gopalswamy, N., Yashiro, S., Akiyama, S. Geoeffectiveness of halo coronal mass ejections. J. Geophys. Res. 112, DOI: 10.1029/2006JA012149, 2007.

Hale, G.E., Ellerman, F., Nicholson, A.H. The Magnetic Polarity of Sun-Spots. Astrophys. J. 49, 153-178, 1919.

Lara, A. The Source Region of Coronal Mass Ejections. Astrophys. J. 688, 647-656, 2008.

McIntosh, P.S. The classification of sunspot groups. Solar Phys. 125, 251-267, 1990.

Michalek, G., Gopalswamy, N., Yashiro, S. A New Method for Estimating Widths, Velocities, and Source Location of Halo Coronal Mass Ejections. Astrophys. J. 584, 472-478, 2003.

Michalek, G., Gopalswamy, N., Lara, A.,Yashiro, S. Properties and geoeffectiveness of halo coronal mass ejections. Space Weather, 4, CiteIDS10003, 2006.

Rust, D.M., Kumar, A. Evidence for Helically Kinked Magnetic Flux Ropes in Solar Eruptions. Astrophys. J. 464, L199-L202, 1996.

Smith, S.F., Howard, R. Structure and Development of Solar Active Regions. IAU Sym. II , ed. Kiepenheuer, O., Dordrecht, D. Reidel., 33, 1967.

Tousey, R. The solar corona. In: Space Res. XIII, Berlin, Akademik-Verlagen, (ed. Rycroft, M.J., Runcorne, S.K.), Berlin, Akademie-Verlag, 713-730, 1973.

Waldmeier, M. Publ. Zurich Obs. 9, 1, 1947.